Hexagonal spike clusters for some PDE's in 2D

Theodore Kolokolnikov* and Juncheng Wei†

*Department of Mathematics and Statistics, Dalhousie University, Halifax, Canada and
†Department of Mathematics, University of British Columbia, Vancouver, Canada

We study hexagonal spike cluster patterns for Gierer-Meinhardt reaction-diffusion system with a precursor on all of $\mathbb{R}^2$. These clusters consist of N spikes which form a nearly hexagonal lattice of a finite size. The lattice density is locally nearly constant, but globally non-uniform. We also characterize a similar hexagonal spike cluster steady state for a simple elliptic PDE $0 = \Delta u - u + u^2 + \varepsilon |x|^2$ with a small "confinement well" $\varepsilon |x|^2$. The key idea is to explicitly exploit the local hexagonality structure to asymptotically approximate the solution using certain lattice sums. In the limit of many spikes, we derive the effective spike density as well as the cluster radius. This effective density is a solution to a certain separable first-order ODE coupled to an integral boundary condition.

1.   INTRODUCTION

Solutions of two-dimensional reaction-diffusion systems often exhibit hexagonally-arranged patterns. In this paper we study a class of nonlocal problems in two dimensions that play an important role in pattern formation in PDE's and formation of hexagonal spike clusters. Our main motivation is to study two-dimensional spike clusters in the Gierer-Meinhardt reaction-diffusion system [1], in the limit where the number of spikes is large. We consider the following version of the GM system on all of $\mathbb{R}^2$ [1–3],

$$a_t = \varepsilon^2 \Delta a - \mu(x)a + \frac{a^2}{h}, \qquad 0 = \Delta h - h + \frac{a^2}{\varepsilon^2}, \quad x \in \mathbb{R}^2 \tag{1.1}$$

Here, a and h represent activator and inhibitor concentrations, respectively, and we make the standard assumption that the activator diffuses much faster than the activator, that is $\varepsilon^2 \ll 1$. The function $\mu(x)$ is called a precursor [1], and spike clusters form near the minimum of $\mu(x)$ [1–5]. A typical choice for $\mu(x)$ that we will use for illustration is

$$\mu(x) = 1 + \alpha |x|^2, \quad \alpha > 0. \tag{1.2}$$

A typical spike cluster, computed using full numerical simulations of (1.1), is shown in Figure 1, corresponding to steady-state of (1.1). The spikes form an almost-regular hexagonal lattice, but whose density is non-uniform. Our goal is to describe this steady state analytically in the limit of large N, including the radius of the cluster and its internal density. In particular, we will derive the effective spike density and spike heights (see also comparison to analytical results in Figure 4). This extends in part the results in [5] from one dimension to two dimensions.

(a)   (b)   (c)   (d)
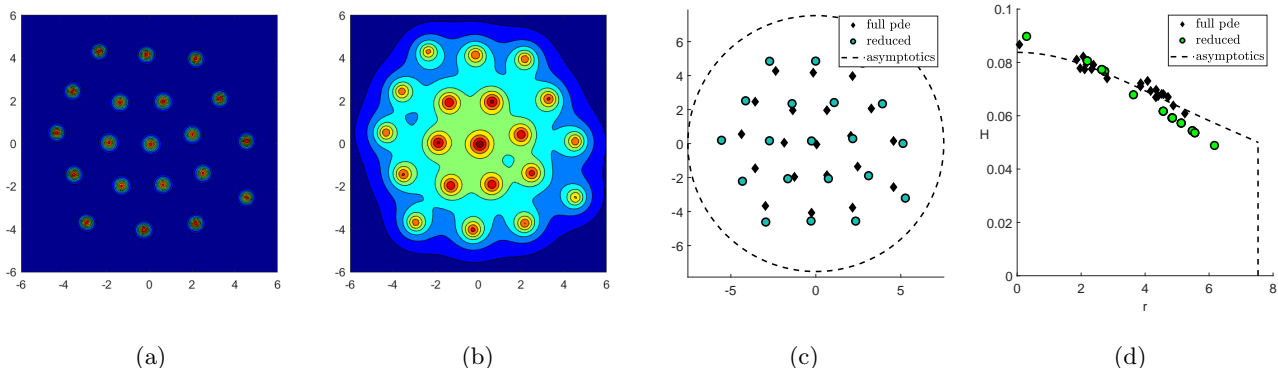
FIG. 1. Cluster steady-state solution to (1.1) consisting of 20 spikes. Contour plot of a and h are shown in (a) and (b) respectively. Parameter values are $\varepsilon = 0.15$ and $\mu(x) = 1 + 0.02 |x|^2$. Computational domain was taken to be $x \in (-15, 15)^2$; increasing the computational domain did not change spike locations. (c): Centers of spikes from the PDE simulation compared with centers generated by the reduced system (4.15). Dashed line denotes spike boundary computed asymptotically from (4.17). (d): Spike height $h(x_j)$ versus $|x_j|$. Comparison between full numerical simulation, the reduced system (4.15) and theoretical prediction (4.17).

As a warmup problem, we consider multi-spike solutions of the single elliptic PDE

$$0 = \Delta u - u + u^2 + \varepsilon |x|^2 \tag{1.3}$$

in either one or two dimensions. Here, $\varepsilon |x|^2$ is a small modulation ($\varepsilon \ll 1$) of the zero background state which acts as a confinement well. This problem – with zero ε – has a very long history and was studied extensively by many authors, see for example [6, 7] and references therein. The ground state consists of multiple spikes. Their locations satisfy a set of algebraic equations that have the form

$$ax = -\nabla_{x_k} \left(\sum K(|x_j - x_k|) \right) \tag{1.4}$$

where $K(r) = e^{-r}$ in 1D and $K(r) = K_0(r)$ (Bessel K0) in 2d, and where a is an $O(\varepsilon)$ constant (see Appendix A).

The key to our computations is that the kernel $K(r)$ decays rapidly; its decay is sufficiently fast so that the summation can be expanded in Taylor series locally.

2.   SPIKE CLUSTERS FOR ELLIPTIC PDE (1.3) IN 1D

We start with the warmup problem (1.3) in one dimension. As shown in Appendix A, in the limit $\varepsilon \to 0$, the steady state to (1.3) consists of N spikes whose centers x_j satisfy an algebraic system

$$\sum_{j \neq k} e^{-|x_k - x_j|} \frac{x_k - x_j}{|x_k - x_j|} \sim ax_k, \quad k = 1 \dots N, \tag{2.5}$$

where $a = \varepsilon/6$.

In the limit of large N, we parametrize: $x_k = x(s)$, where $k = s \in [1, N]$. We then expand in Taylor series,

$$x_{k+l} = x(s+l) = x(s) + x_s l + \frac{x_{ss}}{2} l^2 + \dots$$

$$x_j - x_k = x_s l + \frac{x_{ss}}{2} l^2 \text{ where } l = j - k;$$

$$|x_k - x_j| = x_s |l| + \frac{x_{ss}}{2} l |l| \quad (\text{since } x_s > 0).$$

Define

$$u := \frac{dx}{ds} \approx x_{s+1} - x_s \tag{2.6}$$

which measures the spike inter-distance. For a general $F(r)$, we expand $F(|x_k - x_j|)(x_j - x_k)$ to two orders as follows:

$$F(|x_k - x_j|)(x_j - x_k) \sim F(|ul|)ul + x_{ss} \left(\frac{1}{2} l^2 F(|ul|) + \frac{1}{2} l^2 |l| u F'(|ul|) \right)$$

Using the fact that $x_{ss} = u_x u$, we obtain an approximation

$$\sum_{j \neq k} F(|x_k - x_j|)(x_j - x_k) \sim u_x \phi(u) \tag{2.7}$$

where

$$\phi(u) := \sum_{l=1}^{\infty} u l^2 \left(F(|ul|) + lu F'(|ul|) \right) \tag{2.8}$$

Upon using $F(r) = e^{-r}/r$, we obtain

$$\phi(u) = -\sum_{l=1}^{\infty} u l^2 e^{-ul} = -u \frac{e^{-u}(e^{-u} + 1)}{(1 - e^{-u})^3}. \tag{2.9}$$
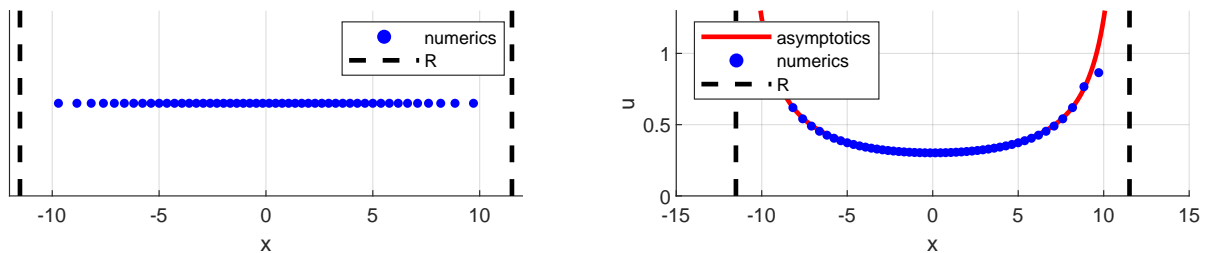
FIG. 2. Left: steady state solution to the one-dimensional equation (2.5). Right: inter-spike spacing, comparison between asymptotics (2.10) and the steady state of (2.5) computed numerically. Parameters are $a = 0.1$ and $N = 50$.

We finally obtain the ODE for the inter-spike distance $u(x)$:

$$\frac{du}{dx} u \frac{e^{-u}(e^{-u}+1)}{(1-e^{-u})^3} \sim ax, \tag{2.10a}$$

The solution to (2.10a) blows up in finite time at some point $x = R$. The density is given by $\rho = 1/u$, so that

$$\int_{-R}^{R} \frac{1}{u} dx = N; \quad \text{where} \quad u(\pm l) = \infty. \tag{2.10b}$$

This integral constraint along with the ODE (2.10a) fully determines $u(x)$. To actually solve for $u(x)$, we simply integrate (2.10a) numerically starting with an initial condition $u(0) = u_0$, then adjust u_0 until the integral constraint is satisfied. Figure 2 shows excellent agreement between the ODE (2.10) and the inter-spike distance obtained by solving (2.5) numerically. To compute the numerical solution to (2.5), note that it corresponds to the steady state of the ODE system

$$\frac{dx_k}{dt} = -ax_k + \sum_{j \neq k} e^{-|x_k - x_j|} \operatorname{sign}(x_k - x_j), \quad k = 1 \ldots N. \tag{2.11}$$

We used the Euler method to evolve (2.11) until its steady state is reached.

We remark that the ode (2.10a) has an implicit solution

$$\frac{1}{e^u - 1} + \frac{ue^u}{(e^u - 1)^2} = \frac{a}{2} \left(R^2 - x^2 \right), \tag{2.12}$$

although the integral in (2.10b) does not appear to have an explicit form. For this reason, we used simple Euler method to integrate (2.10a) directly to generate the continuum curve in Figure 2.

Finally, consider the scaling $x = \beta \hat{x}$. Substituting into (2.10), let $\hat{a} = a\beta^2$, $\hat{R} = R/\beta$, $\hat{N} = N/\beta$. Then the system (2.10) is invariant under this scaling after dropping the hats. In other words, if we double N, we can quarter a and retain the same spike density but on the domain double the size.

3. SPIKE CLUSTERS FOR ELLIPTIC PDE (1.3) IN 2D

We now consider the cluster solutions of (1.3) in two dimensions. As shown in Appendix A, the spike centers satisfy an algebraic system

$$\sum_{j \neq k} K_1(|x_k - x_j|) \frac{x_k - x_j}{|x_k - x_j|} = ax_k. \tag{3.13}$$

where $a \approx 0.13 \, \varepsilon$. Figure 3 shows a typical two-dimensional solution of (3.13). As in 1D, the solution to (3.13) is computed by evolving the associated ODE whose steady state satisfies (3.13). Numerics indicate that this steady state has a hexagonal latttice structure. While the *overall* density is clearly non-uniform, the *local* structrue is still nearly hexagonal. Motivated by the numerics, we make a couple of key assumptions: (a) the lattice structure is nearly-hexagonal at every position x_k; (b) the steady state is nearly radially symmetric in the limit of large N. To
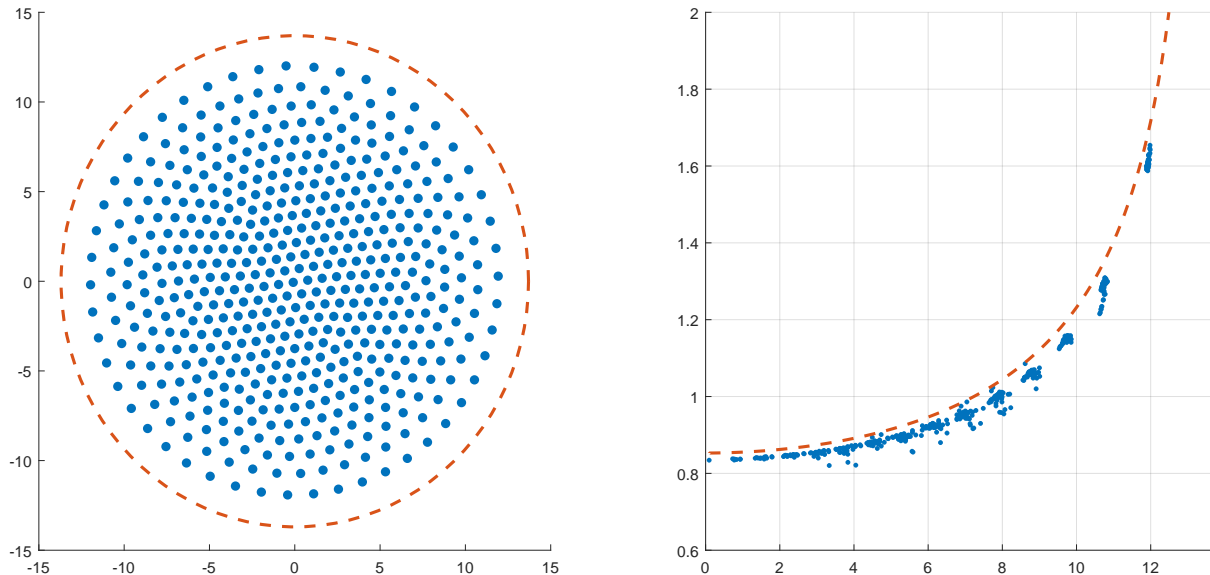
FIG. 3. LEFT: steady state for (3.13) with $N = 500$ and $a = 0.1$. Dots represent the steady state x_j. Dashed line represents the theoretical boundary of the steady state in the continuum limit $N \gg 1$. RIGHT: scatter plot of the average distance $u(x_j)$ from a point to any of its neighbours, as a function of $|x_j|$. Solid curve is the analytical prediction of the continuum limit as given by equations (3.14).

this end, in analogue to the one-dimensional problem, we define $u(x_k)$ to be the lattice spacing at x_k, that is, the distance from x_k to its closest neighbour:

$$u(x_k) = \min_{j \neq k} |x_j - x_k|.$$

Assuming near radial symmetry, we write $u(x_k) \sim u(r)$, $r = |x_k|$. In Appendix C we then derive the following approximation:

$$\sum_{j \neq k} -K_1(|x_k - x_j|)\frac{x_k - x_j}{|x_k - x_j|} \sim u_r \phi_2(u)$$

where ϕ_2 is given in (5.29). Therefore we obtain the ODE for lattice spacing:

$$\frac{du}{dr}\phi_2(u) = -ar \tag{3.14a}$$

As in one-dimension, we assume the lattice has radius R with $u(r) \to \infty$ as $r \to R^-$. Since there are in total N lattice points, the analogue of (2.10b) for a two-dimensional hexagonal lattice then becomes

$$N = \frac{2}{\sqrt{3}} \int_0^R \left(\frac{1}{u(r)}\right)^2 2\pi r dr. \tag{3.14b}$$

We then solve (3.14a) subject to the constraint (3.14b) to obtain the lattice spacing $u(r)$ as well as the lattice radius R. Figure 3 illustrates a very good agreement between the continuum limit (3.14) and the full simulation of (3.13).

As in 1D, let's examine how the density changes with a. By scaling $r = \beta \hat{r}$ and letting $\hat{a} = a\beta^2$, $\hat{R} = R/\beta$, $\hat{N} = N/\beta^2$, the equations (3.14) remain invariant after dropping the hats. In other words, if we double N, we can half a and retain the same spike density but on a domain that has twice the area (whose radius is $\sqrt{2}$ larger).
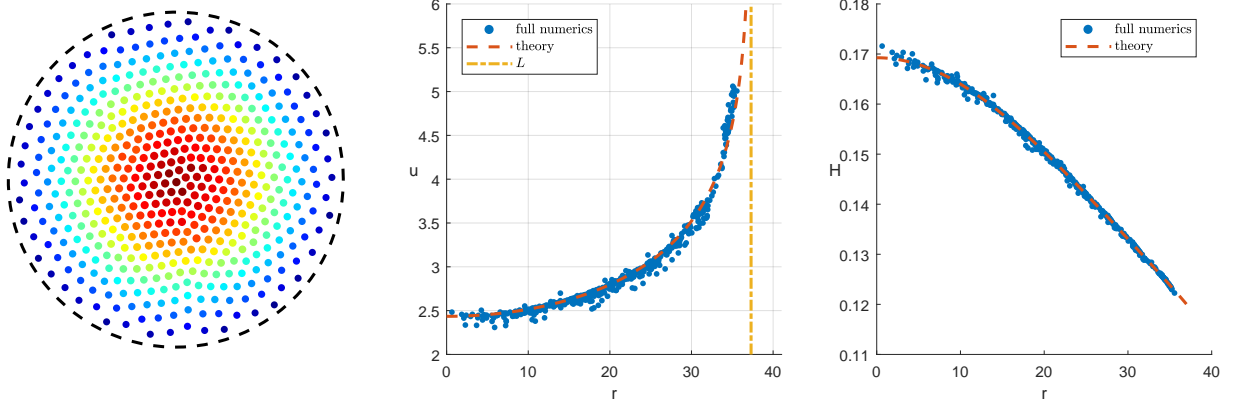
FIG. 4. LEFT: Steady state for (4.15) with $N = 500$, $\mu(x) = 1 + 0.025x^2$ and $\varepsilon = 0.08$. Dots represent the steady state x_j; their size and colour are proportional to H_j. Dashed line represents the theoretical boundary of the steady state in the continuum limit $N \gg 1$. MIDDLE: scatter plot of the average distance $u(x_j)$ from a point to any of its neighbours, as a function of $|x_j|$. Solid curve is the analytical prediction of the continuum limit as given by (4.17). RIGHT: Scatter plot of the H_j as a function of $|x_j|$ and comparison to theory.

4. SPIKE CLUSTERS FOR GM MODEL IN 2D

We now consider study spike density for the GM system (1.1) in two dimensions. In Appenedix B, we derive the following reduced system for a steady state consisting of N spikes:

$$H_k \sim \mu_k H_k^2 \frac{\int w^2}{2\pi} \log \varepsilon^{-1} + \sum_{j \neq k} \mu_j H_j^2 K_0 \left(|x_k - x_j| \right) \frac{\int w^2}{2\pi} \tag{4.15a}$$

$$0 = \frac{\nabla \mu_k}{\mu_k} \frac{1}{2} + \frac{1}{H_k} \sum_{j \neq k} \mu_j H_j^2 K_0' \left(|x_k - x_j| \right) \frac{x_k - x_j}{|x_k - x_j|} \frac{\int w^2}{2\pi} \tag{4.15b}$$

Here, x_j is the location of j-th spike and $\mu_j = \mu(x_j)$ and $H_j \sim h(x_j)$.

$$H_k \alpha = \frac{\mu_k H_k^2}{\eta} + \sum_{j \neq k} \mu_j H_j^2 K_0 \left(|x_k - x_j| \right),$$

$$0 = \frac{\nabla \mu_k}{2\mu_k} \alpha + \frac{1}{H_k} \sum_{j \neq k} \mu_j H_j^2 K_0' \left(|x_k - x_j| \right) \frac{x_k - x_j}{|x_k - x_j|}$$

where $\alpha = \frac{2\pi}{\int w^2}$

We start with estimating

$$\sum_{j \neq k} \mu_j H_j^2 K_0 \left(|x_k - x_j| \right) \sim \mu(r) H^2(r) \phi_1(u)$$

where ϕ_1 is given in Appendix C, equation (5.28). We therefore obtain

$$H(x) \sim \frac{\alpha}{\left(\log \varepsilon^{-1} + \phi_1(u(x)) \right)} \frac{1}{\mu(x)} \tag{4.16}$$

Applying identity (5.27) from Appendix C we approximate

$$\sum_{j \neq k} \mu_j H_j^2 K_0' \left(|x_k - x_j| \right) \frac{x_j - x_k}{|x_j - x_k|} \sim \mu H^2 u_r \phi_2(u) + \left(\mu H^2 \right)_r \phi_3(u)$$

so that

$$\mu H^2 u_r \phi_2 + \left(\mu_r H^2 + 2\mu H H_r\right)\phi_3 = H \frac{\mu'(r)}{2\mu(r)} \frac{2\pi}{\int w^2}$$

Upon substituting (4.16) and simplifying we finally obtain

$$u'(r) = \frac{\mu'(r)}{\mu(r)} f(u) \tag{4.17a}$$

where

$$f(u) := \frac{\left(\phi_3(u) + \left(\phi_1(u) + \log \varepsilon^{-1}\right)/2\right)\left(\log \varepsilon^{-1} + \phi_1(u)\right)}{\left(\left(\log \varepsilon^{-1} + \phi_1(u)\right)\phi_2(u) - 2\phi_1'(u)\phi_3(u)\right)} \tag{4.17b}$$

As in Section 3, we seek solutions to (4.17a) which blow up at some point $r = R$, and we suppliment this ODE by the density constraint given by

$$N = \frac{2}{\sqrt{3}} \int_0^R \left(\frac{1}{u(r)}\right)^2 2\pi r dr; \qquad u(r) \to \infty \text{ as } r \to R^-. \tag{4.17c}$$

Together, equations (4.17) constitute the continuum limit of large N for the reduced system (4.15).

Figure 5 shows the plot of the function $f(u)$ with $\varepsilon = 0.15$. It has a pole, and is increasing to the right of its right-most root, which we denote by $u_{\min}$. As a result, it is easy to see that the solution to (4.17) exists for *any* N, with $u(r) \geq u_{\min}$.
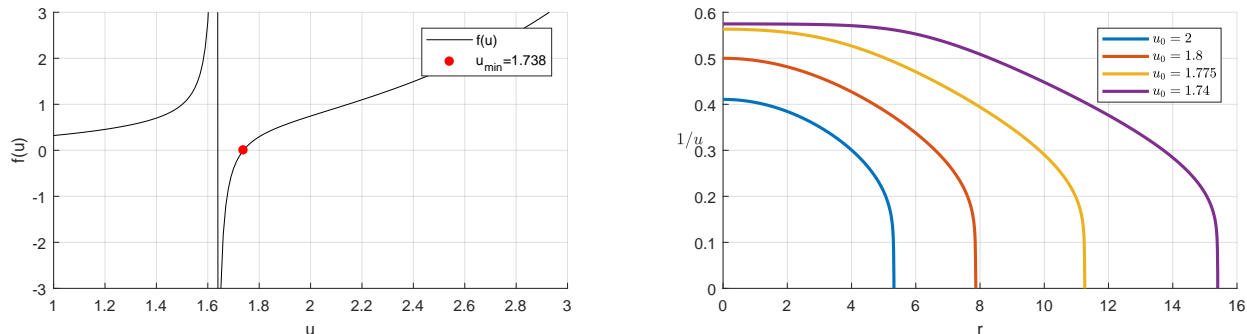
FIG. 5. u and f

Figure 4 illustrates an excellent agreement between the continuum limit (4.17) and direct numerical solution of the reduced system 4.15.

5. DISCUSSION

In this paper, we derived the continuum-limit description of the cluster steady state for the Gierer-Meinhardt model in two dimension. In our computation, we made a key assumption that the lattice structure is *locally nearly hexagonal,* and we explicitly used this assuimption when summing up the relevant sums. A different lattice structure (say square) would lead to different spike density. The hexagonality of the lattice is based purely on observing numerical simulations. It remains an open question to rigorously show that the lattice structure is indeed locally hexagonal.

Recently in [8, 9], the two-dimensional lattice density for vortices in BEC was derived. The analysis there relies on integral equations, and the results do not depend on the local structure of the lattice (even it it does happen to be hexagonal). It also borrows *nonlocal* techniques developed recently in the context of aggregation model of biological swarming; see e.g. [10–13] and references therein. By contrast, our derivations expand the lattice structure *locally* and make explicit use of the hexagonal lattice structure.

Even though the analysis and results here are completely different, the systems we considered in this paper are closely related to some of the recent work in the swarming literature. For instance equation (2.11) is exactly the same model as was considered in the paper [11] (see equation (3.1) there), but with a very different scaling: in our

context, the constant a is very small and scales like $1/N^2$, while the radius of the swarm scales like N. By contrast, the analysis [11] applies when a is $O(1)$, and the resulting swarm has $O(1)$ radius *independent* of N. To borrow the nomenclature from the swarming/statistical physics literature [14, 15], the latter corresponds to the "confining" (or "catastrophic") regime while the former is "H-stable". The steady states we analyze here fall into the "H-stable" regime due to a very weak contributions of the far-away neighbours, and requires an alltogether different analysis.

In a recent paper [5], we analysed a one-dimensional cluster solution for the GM model. There, a one-dimesional analogue of equations (4.17) was derived. The key difference is that a 1D steady state disappeared for sufficiently large N. In other words, there was a *maximum* $N = N_{\max}$ for which the continuum solution was possible. By contrast, the continuum limit in two dimensions appears to exist for arbitrary large N. However numerical simulations of the full PDE system (1.1) show that if N is too large, spikes disappear through what appears to be a competition instability [16, 17]. So far we were unsuccessful in deriving the critical thresholds for stability. This is a key open problem for future research.

Finally, we have assumed in our analysis that $\mu(x)$ is radially symmetric, which leads to (nearly) radially symmetric spike clusters. It would be very interesting to extend our analysis to the case of non-radially symmetric $\mu(x)$, which leads to non-radial clusters.

APPENDIX A: MULTISPIKE GROUND STATES FOR A SINGLE PDE

We start by deriving the reduced system for a PDE

$$0 = \Delta u - u + u^2 + \varepsilon f(x) \tag{5.18}$$

with an arbitrary function $f(x)$, assuming that ε is small. The computation is relatively standard, see for example [6].

We assume that u has the form

$$u = \sum_j w(x - x_j) + R$$

where $R \ll 1$, with $w(y)$ being the ground-state solution satisfying

$$\Delta w - w + w^2 = 0, \quad w(y) \to 0 \text{ as } |y| \to \infty. \tag{5.19}$$

It is well-known that the solution to (5.19) is unique, and $w(y)$ decays exponentially as $|y| \to \infty$.

Assume that x_j For x near x_k, let $y = x - x_k$. We then obtain

$$0 \sim \Delta R - R + 2w_k R + f(y + x_k) + \sum_{j \neq k} 2w(x - x_k)w(x - x_j).$$

Multiply by $\nabla w_k(x - x_k)$ and integrate to obtain

$$0 \sim \int \varepsilon \nabla_y w(y) f(y + x_k) dy + \sum_{j \neq k} \int 2w(x - k_k)\nabla w(x - x_k)w(x - x_j) dx.$$

Simplify

$$\int f(y + x)\nabla w(y) = -\int \nabla f(y + x)w(y) dy$$

and evaluate

$$\int 2w(x - x_k)\nabla_{x_k} w(x - x_k)w(x - x_j) dx = -\nabla_{x_k} \int w^2(x - x_k)w(x - x_j) dx$$

and furthermore,

$$\int w^2(x - x_k)w(x - x_j) dx \sim \int w^2(y)w(y + d) dx, \text{ where } d = x_k - x_j. \tag{5.20}$$

Next we simplify (5.20), in one or two dimensions.

One dimesion. For large $|d|$, we have $w(y+d) \sim 6e^{-|d|}e^{-y}$ so that

$$\int w^2(y)w(y+d)dx \sim 6e^{-|d|}\int w^2 e^{-y} = 6e^{-|d|}\int (w-w'')e^{-y} = 6e^{-|d|}(w'+w)e^{-y}|_{-\infty}^{\infty} = 72e^{-|d|}. \tag{5.21}$$

In conclusion, we obtain, in 1D,

$$0 \sim -\varepsilon \int f'(y+x)w(y)dy - 72\sum_{j\neq k}\frac{d}{dx_k}\left(e^{-|x_k-x_j|}\right). \tag{5.22}$$

Finally suppose that $f(x) = x^2$. Then $\int f'(y+x)w(y)dy = 12\varepsilon x$ and (5.22) becomes (2.5) with $a = \varepsilon/6$.

Two dimensions. To simplify (5.20) in 2D, assume $|d| \gg 1$ and expand in the far-field,

$$w(y+d) \sim B_0 |y+d|^{-1/2}e^{-|y+d|}.$$

The constant $B_0 \approx 10.7$ is estimated by numerically evaluating $B_0 \approx w(r)r^{1/2}e^r$ for large r (say $r = 10$). We then estimate

$$\int w^2(y)w(y+d)dx \sim |d|^{-1/2}e^{-|d|}B_0\int w^2(y)e^{-y_1}dy$$

The integral $\int w^2(y)e^{-y_1} \approx 54.45$ is also evaluated numerically. We thus obtain

$$\int w^2(y)w(y+d)dx \sim C_0 K_0(|d|), \quad |d| \gg 1$$

where

$$C_0 = \frac{1}{\sqrt{\pi/2}}B_0\int w^2(y)e^{-y_1}dy \approx 464.84.$$

(we used $K_0(r) \sim (\pi/2)^{1/2}r^{-1/2}e^{-r}$ for large r). In summary, we obtain

$$0 \sim -\varepsilon\int \nabla f(y+x)w(y)dy - C_0\nabla_{x_k}\sum_{j\neq k}K_0(|x_k-x_j|). \tag{5.23}$$

Finally, for $f(x) = |x|^2$, we evaluate $\int \nabla f(y+x)w(y)dy = 2x\int w(y)dy$. Then (5.23) yields (3.13) with $a = \frac{2\int w(y)}{C_0}\varepsilon \approx 0.13\,\varepsilon$.

APPENDIX B: REDUCED SYSTEM FOR MULTIPLE SPIKES IN GM MODEL

Here, we derive the reduced equations of motion the GM model (1.1). This calculation is relatively standard, see for example [18–20], and we include it here for completeness. We consider a solution to (1.1) that consists of N "spikes", corresponding to delta-type concentrations of the activator. The reduced system consists of $2N$ ODE's for spike centers coupled to N algebraic equations related to spike heights.

Let x_k, $k = 1 \ldots n$ be the centers of N spikes. Near the spike k, we expand

$$a = U(y) + \varepsilon W(y) + O\left(\varepsilon^2\right)$$
$$h = H(y) + \varepsilon P(y) + O\left(\varepsilon^2\right)$$

where

$$y = \frac{x - x_k(\varepsilon^2 t)}{\varepsilon}.$$

At leading order we get

$$0 = \Delta U - \mu_k U + U^2/H$$
$$0 = \Delta H$$

Then H is constant obtained via matching to the outer region and we obtain

$$H \sim H_k, \quad U = H_k \mu_k w(\sqrt{\mu_k} y), \tag{5.24}$$

where $\mu_k = \mu(x_k)$; H_k will be obtained via matching to outer region below, and w is the ground state satisfying

$$\Delta w - w + w^2 = 0; \quad w \text{ is radially symmetric}; \quad w(y) \to 0 \text{ as } |y| \to \infty. \tag{5.25}$$

To determine H_k and P, we match to the outer region. We write

$$h(x) \sim \sum G(x, x_j) S_j$$

Here, $G(x, x_j)$ is the Green's function satisfying

$$\Delta G - G + \delta(x - x_j) = 0, \quad x, x_j \in \mathbb{R}^2$$

and

$$S_j = H_j^2 \mu_j \int_{\mathbb{R}^2} w^2(z) dz.$$

Recall that

$$G(x, x_j) = \frac{1}{2\pi} K_0(|x - x_j|)$$

with the singularity behaviour

$$G(x, x_j) = -\frac{1}{2\pi} \log |x - x_j| + \frac{\log 2 - \gamma}{2\pi} + o(|x - x_j|).$$

Expanding h to two orders and matching to H_k and P we then obtain

$$H_k = \sum_j H_j^2 \mu_j G_{kj} \int w^2$$

$$P = y \cdot \sum_j H_j^2 \mu_j \nabla G_{kj} \int w^2$$

Here,

$$G_{kj} = \begin{cases} \frac{1}{2\pi} K_0(|x_k - x_j|), & \text{if } k \neq j \\ \frac{1}{2\pi} \log \varepsilon^{-1} + \frac{\log 2 - \gamma}{2\pi}, & \text{if } k = j \end{cases},$$

$$\nabla G_{kj} = \begin{cases} \frac{1}{2\pi} K_0'(|x_k - x_j|) \frac{x_k - x_j}{|x_k - x_j|}, & \text{if } k \neq j \\ 0, & \text{if } k = j \end{cases}$$

Next-order equations are

$$-x_k' \nabla_y U = \Delta W - \mu_k W - U y \cdot \nabla \mu_k + 2W \frac{U}{H_k} - \frac{U^2}{H_k^2} P$$

where $\nabla \mu_k = \nabla \mu(x_k)$. Multipy by ∇U_0 and integrate to obtain:

$$-x_0' \int |\nabla U|^2 = -\int y \cdot \nabla \mu_k U \nabla U - \int \frac{U^2}{H^2} P \nabla U$$

$$= \nabla \mu_k \int \frac{U^2}{2} + \frac{1}{3H_k^2} \int U^3 \nabla P$$

Using the identities [18]:

$$\frac{\int w^3}{\int w^2} = 3, \quad \frac{\int |\nabla w|^2}{\int w^2(z) dz} = 1/2, \quad \int w^2 = 31.04,$$

we obtain

$$-\frac{x_k'(\varepsilon^2 t)}{2} = \frac{1}{2}\frac{\nabla \mu_k}{\mu_k} + H_k^{-1}\nabla P.$$

so that the steady state satisfies

$$0 = \frac{1}{2}\frac{\nabla \mu_k}{\mu_k} + H_k^{-1}\sum_j H_j^2 \mu_j \nabla G_{kj}\int w^2$$

$$H_k = \sum_j H_j^2 \mu_j G_{kj}\int w^2$$

APPENDIX C: ESTIMATING LATTICE SUMS

The sum $\sum_{j\neq k} S_j K_0\left(|x_k - x_j|\right).$
Assume that near x_k, the points x_j are given by

$$x_j \sim x_k + ul, \text{ where } l = l_1 + e^{i\pi/3}l_2, \quad (l_1, l_2)\in\mathbb{Z}^2.$$

Here, $u > 0$ is distance from the center x_k to its six neighbours. We then estimate

$$\sum_{j\neq k} S_j K_0\left(|x_k - x_j|\right)\sim S(x_k)\phi_1(u),$$

where

$$\phi_1(u) = \sum_{j\neq k}K_0\left(u\,|l|\right)$$

The sum $\sum_{j\neq k} S\left(x_j\right) F\left(|x_j - x_k|\right)\left(x_j - x_k\right),$ where $F(r) = K_0'(r)/r.$
Assume that near x_k, the points x_j are given by

$$x_j = x_k + ul + \varepsilon l^2, \quad\text{where } |\varepsilon| \ll 1 \text{ and } l = l_1 + e^{i\pi/3}l_2, \quad (l_1, l_2)\in\mathbb{Z}^2$$

That is: (a) the lattice is locally nearly hexagonal; (b) Locally, the lattice is a small conformal deformation of a perfect hexagonal lattice. Because of radial symmetry, we may further assume without loss of generality, that x_k lies on the real axis and ε is real. Expanding to two orders we have

$$|x_j - x_k| = u\,|l| + \varepsilon\,|l|\,\mathrm{Re}(l)$$
$$F\left(|x_j - x_k|\right)\left(x_j - x_k\right) = \left(F\left(u\,|l|\right) + \varepsilon\,|l|\,\mathrm{Re}(l)F'\left(u\,|l|\right)\right)\left(ul + \varepsilon l^2\right)$$
$$= ulF\left(u\,|l|\right) + \varepsilon\left[l^2 F\left(u\,|l|\right) + |l|\,\mathrm{Re}(l)ulF'\left(u\,|l|\right)\right]$$

and

$$S(|x_j|)\sim S(r) + u\,\mathrm{Re}\left(l\right)S'(r)$$

where $r = |x_k|$. Therefore

$$S(x_j)F\left(|x_j - x_k|\right)\left(x_j - x_k\right) = S(r)ulF\left(u\,|l|\right) + \varepsilon S\left(x\right)\left[l^2 F\left(u\,|l|\right) + |l|\,\mathrm{Re}(l)ulF'\left(u\,|l|\right)\right] + u\,\mathrm{Re}\left(l\right)S'(r)ulF\left(u\,|l|\right)$$

and summing over all l we obtain

$$\sum_{j\neq k} S\left(x_j\right) F\left(|x_j - x_k|\right)\left(x_j - x_k\right)\sim \varepsilon S\left(r\right)\sideset{}{'}\sum\left[l^2 F\left(u\,|l|\right) + |l|\,\mathrm{Re}(l)ulF'\left(u\,|l|\right)\right] + S'(r)\sideset{}{'}\sum u^2\,\mathrm{Re}\left(l\right)lF\left(u\,|l|\right)$$

where $\sum'$ denotes the double sum $(l_1, l_2)\in\mathbb{Z}^2\backslash\left\{(0, 0)\right\}.$
Finally, we have:

$$\varepsilon = \frac{1}{2}\frac{du}{dl} = \frac{1}{2}\frac{du}{dr}\frac{dr}{dl} = \frac{1}{2}u_x u$$

We therefore conclude:

$$\sum_{j \neq k} S\left(x_j\right) F\left(\left|x_j - x_k\right|\right)\left(x_j - x_k\right) = S'(r)\phi_3(u) + S\left(r\right) u_x \phi_2(u)$$

where

$$\phi_3(u) = u^2 \sum \operatorname{Re}\left(l\right) l F\left(u\left|l\right|\right)$$

$$\phi_2(u) = \frac{u}{2} \sum \left[l^2 F\left(u\left|l\right|\right) + l \operatorname{Re}(l)\left|l\right| u F'\left(u\left|l\right|\right)\right]$$

Substituting $F(r) = \frac{K'(r)}{r}$ and simplifying using $K''(r) = K(r) - K'(r)/r$ then yields

$$l^2 F\left(u\left|l\right|\right) + l \operatorname{Re}(l)\left|l\right| u F'\left(u\left|l\right|\right) = l^2 \frac{K'(r)}{r} + l \operatorname{Re}(l) r \left(K'/r\right)'$$

$$= -\left|l\right|^2 K'(r)/r + l \operatorname{Re}(l) K(r)$$

In summary,

$$\sum_{j \neq k} S_j K_0\left(\left|x_k - x_j\right|\right) \sim S(x_k)\phi_1(u), \tag{5.26}$$

$$\sum_{j \neq k} S\left(x_j\right) K_0'\left(\left|x_j - x_k\right|\right) \frac{x_j - x_k}{\left|x_j - x_k\right|} = S'(r)\phi_3(u) + S\left(r\right) u_x \phi_2(u) \tag{5.27}$$

where

$$\phi_1(u) = \sum_{j \neq k} K_0\left(u\left|l\right|\right) \tag{5.28}$$

$$\phi_2(u) = \frac{1}{2} \sum \left[-\left|l\right| K_0'(u\left|l\right|) + ul \operatorname{Re}(l) K_0(u\left|l\right|)\right] \tag{5.29}$$

$$\phi_3(u) = u \sum \operatorname{Re}\left(l\right) \frac{l}{\left|l\right|} K_0'\left(u\left|l\right|\right), \tag{5.30}$$

$$\phi_1'(u) = \sum_{j \neq k} \left|l\right| K_0'\left(u\left|l\right|\right). \tag{5.31}$$

[1] A. Gierer, H. Meinhardt, A theory of biological pattern formation, Kybernetik 12 (1) (1972) 30–39.
[2] D. Iron, M. J. Ward, J. Wei, The stability of spike solutions to the one-dimensional gierer–meinhardt model, Physica D: Nonlinear Phenomena 150 (1) (2001) 25–62.
[3] J. Wei, M. Winter, Stable spike clusters for the one-dimensional gierer–meinhardt system, European Journal of Applied Mathematics 28 (4) (2017) 576–635.
[4] J. Wei, M. Winter, W. Yang, Stable spike clusters for the precursor gierer–meinhardt system in r2, Calculus of Variations and Partial Differential Equations 56 (5) (2017) 142.
[5] T. Kolokolnikov, S. Xie, Spike density distribution for the gierer-meinhardt model with precursor, submitted.
[6] W.-M. Ni, J. Wei, On the location and profile of spike-layer solutions to singularly perturbed semilinear dirichlet problems, Communications on Pure and Applied Mathematics 48 (7) (1995) 731–768.
[7] C. Gui, J. Wei, Multiple interior peak solutions for some singularly perturbed neumann problems, Journal of differential equations 158 (1) (1999) 1–27.
[8] S. Xie, P. G. Kevrekidis, T. Kolokolnikov, Multi-vortex crystal lattices in bose–einstein condensates with a rotating trap, Proc. R. Soc. A 474 (2213) (2018) 20170553.
[9] T. Kolokolnikov, P. Kevrekidis, R. Carretero-González, A tale of two distributions: from few to many vortices in quasi-two-dimensional bose–einstein condensates, Proc. R. Soc. A 470 (2168) (2014) 20140048.
[10] R. C. Fetecau, Y. Huang, T. Kolokolnikov, Swarm dynamics and equilibria for a nonlocal aggregation model, Nonlinearity 24 (10) (2011) 2681.
[11] A. J. Bernoff, C. M. Topaz, Nonlocal aggregation models: A primer of swarm equilibria, SIAM Review 55 (4) (2013) 709–747.
[12] Y. Chen, T. Kolokolnikov, A minimal model of predator–swarm interactions, Journal of The Royal Society Interface 11 (94) (2014) 20131208.
[13] G. Flierl, D. Grünbaum, S. Levins, D. Olson, From individuals to aggregations: the interplay between behavior and physics, Journal of Theoretical biology 196 (4) (1999) 397–454.

[14] M. R. DOrsogna, Y.-L. Chuang, A. L. Bertozzi, L. S. Chayes, Self-propelled particles with soft-core interactions: patterns, stability, and collapse, Physical review letters 96 (10) (2006) 104302.

[15] T. Kolokolnikov, H. Sun, D. Uminsky, A. L. Bertozzi, Stability of ring patterns arising from two-dimensional particle interactions, Physical Review E 84 (1) (2011) 015203.

[16] J. Wei, M. Winter, Spikes for the gierer–meinhardt system in two dimensions: the strong coupling case, Journal of Differential Equations 178 (2) (2002) 478–518.

[17] J. Wei, M. Winter, Existence and stability analysis of asymmetric patterns for the gierer–meinhardt system, Journal de mathématiques pures et appliquées 83 (4) (2004) 433–476.

[18] M. J. Ward, D. McInerney, P. Houston, D. Gavaghan, P. Maini, The dynamics and pinning of a spike for a reaction-diffusion system, SIAM Journal on Applied Mathematics 62 (4) (2002) 1297–1328.

[19] T. Kolokolnikov, M. J. Ward, Reduced wave green's functions and their effect on the dynamics of a spike for the gierer–meinhardt model, European Journal of Applied Mathematics 14 (5) (2003) 513–545.

[20] J. Wei, M. Winter, Stationary multiple spots for reaction–diffusion systems, Journal of mathematical biology 57 (1) (2008) 53–89.